Robust conversion of singlet spin order in coupled spin-1/2 pairs by adiabatically ramped RF-fields

CrossMark

Andrey N. Pravdivtsev [a,b,1], Alexey S. Kiryutin [a,b,1], Alexandra V. Yurkovskaya [a,b], Hans-Martin Vieth [a,c], Konstantin L. Ivanov [a,b,*]

[a] International Tomography Center, Siberian Branch of the Russian Academy of Science, Institutskaya 3A, Novosibirsk 630090, Russia
[b] Novosibirsk State University, Pirogova 2, Novosibirsk 630090, Russia
[c] Institut für Experimentalphysik, Freie Universität Berlin, Arnimallee 14, Berlin 14195, Germany

ARTICLE INFO

ABSTRACT

We propose a robust and highly efficient NMR technique to create singlet spin order from longitudinal spin magnetization in coupled spin-½ pairs and to perform backward conversion (singlet order) → magnetization. In this method we exploit adiabatic ramping of an RF-field in order to drive transitions between the singlet state and the $T_\pm$ triplet states of a spin pair under study. We demonstrate that the method works perfectly for both strongly and weakly coupled spin pairs, providing a conversion efficiency between the singlet spin order and magnetization, which is equal to the theoretical maximum. We anticipate that the proposed technique is useful for generating long-lived singlet order, for preserving spin hyperpolarization and for analyzing singlet spin order in nearly equivalent spin pairs in specially designed molecules and in low-field NMR studies.

1. Introduction

Nuclear singlet states with extended lifetimes [1,2] are becoming a powerful tool in Nuclear Magnetic Resonance (NMR) spectroscopy. Such Long-Lived spin States (LLSs) can be formed in pairs of spins ½: in such spin pairs the singlet spin state is often long-lived for the reason that it is immune to mutual dipolar relaxation, which typically gives the dominant contribution to spin relaxation rates. LLSs lifetimes, T_S, can by far exceed nuclear T_1-relaxation times: for instance, for the β-CH_2 protons of partially deuterated aromatic amino acids they can be as long at $45 \cdot T_1$ [3,4]. Long LLS lifetimes have been found in the ^{15}N-labeled N_2O molecule [5]; recently, T_S of the order of 1 hour for a pair of ^{13}C spins has been reported for specially designed ^{13}C-labeled molecules [6]. LLSs can be sustained once the nuclear singlet state is an eigen-state (or nearly an eigen-state) of the spin Hamiltonian. Such a condition can be fulfilled by placing the spins at a sufficiently low magnetic field [7], by applying strong RF-excitation (spin-locking) [7] or by using specially designed molecules with "nearly-equivalent" pairs of spins [6]. LLSs create a unique resource

for studying slow dynamic processes, notably, for probing slow molecular motions [8,9], slow diffusion and transport [10–14] and drug-screening [15], when fast T_1-relaxation imposes restrictions for the NMR observation window. Another promising application of LLSs is storing non-thermal nuclear spin polarization [16–23]. Such a polarization, often termed hyperpolarization, provides an enormous gain in NMR signal intensity but irreversibly decays due to T_1-relaxation. In such a situation LLSs can be a remedy: the precious hyperpolarization stored in the nuclear spin order often has extended lifetimes.

A prerequisite for utilizing singlet spin order in various NMR applications is a robust method for conversion of spin magnetization into the singlet spin order and back. There has been a number of techniques developed [1], which provide the desired spin order conversion; however, none of them works efficiently for both weakly and strongly coupled spins. In this context, we would like to mention a technique proposed by some of us [24–26], which is based on slowly (adiabatically) switching a spin-locking RF-field to enable highly efficient magnetization-to-singlet (M2S) and singlet-to-magnetization (S2M) conversion. The method is based on correlating nuclear spin states in the RF-rotating frame of reference; it provides excellent conversion efficiency (equal to the maximal theoretical value [27]) and enables suppression of residual NMR signals. Previously, the method has been applied only to weakly coupled spin pairs, i.e., when the coupling strength,

J, is much smaller than the difference, δv, in the NMR frequencies. This can be a limitation of the method as experiments on LLSs are often performed on strongly-coupled spin systems, i.e., in the situation where $|J| \sim \delta v$ or even $|J| \gg \delta v$. The new element of this work is extension of the technique to spin pairs with an arbitrary relation between J and δv. In fact, our method does not have a fundamental limitation with respect to the coupling regime in contrast to other methods, which can be applied either for weakly or strongly coupled spin pairs. With the aim to extend the capabilities of the technique, here we demonstrate that it is a universal method for robust M2S and S2M conversion, which is efficient for an arbitrary spin-½ pair. We term this technique "*Adiabatic-Passage Spin Order Conversion*", or *APSOC*, without regard to the coupling regime. To demonstrate the power of our method we apply it to a peptide having strongly and weakly coupled spin pairs, namely, CH_2-groups. Possible applications of the APSOC technique are discussed.

2. Theory

2.1. Adiabatic correlation of states

Let us describe how APSOC works in a system of two coupled spins upon a perfectly adiabatic RF-field switch. In general, by adiabatic variation of the Hamiltonian we mean the following situation. Let us imagine, that for a time-dependent Hamiltonian $\widehat{H}(t)$ we can solve the eigen problem at any instant of time, i.e., $\widehat{H}(t)|i\rangle = E_i(t)|i\rangle$. Thus, we know the instantaneous energies, $E_i(t)$, and eigen-states, $|i(t)\rangle$. The adiabaticity condition implies that the rates, at which the eigen-states of $\widehat{H}$ change with time, given by the expression $\langle i|\frac{d}{dt}|j\rangle$, are much smaller than the instantaneous frequencies of coherent spin evolution, $\omega_{ij}(t) = (E_i - E_j)$, i.e., $\xi_{ij} = \langle i|\frac{d}{dt}|j\rangle/\omega_{ij} \ll 1$. The ξ_{ij} parameter is the *adiabaticity parameter*; the condition tells us how fast the eigen-states of $\widehat{H}$ change as compared to the frequency of internal evolution of the spin system. In the situation $\xi_{ij} \ll 1$ state populations follow the time-dependent states. Hence, we simply need to correlate the states before and after the switch. In such a situation the switch becomes reversible. This means that, if we know, for instance, how magnetization is converted into the singlet spin order by turning on an RF-field, we also know how the singlet state population is converted to magnetization by turning off an RF-field. Thus, it is sufficient to correlate the spin states in the rotating frame for zero RF-field strength and under a strong RF-field.

The Hamiltonian of two coupled spins (spin "a" and spin "b") in an external magnetic field B_0 directed along the z-axis and an oscillating RF-field directed along the x-axis in the laboratory frame is as follows (as written in the units of h):

$$\widehat{H}^{lf} = -v_a \widehat{I}_{az} - v_b \widehat{I}_{bz} - 2v_1 \cos(2\pi v_{rf} t) \cdot (\widehat{I}_{ax} + \widehat{I}_{bx}) + J(\widehat{\mathbf{I}}_a \cdot \widehat{\mathbf{I}}_b) \quad (1)$$

Here $\widehat{\mathbf{I}}_a$ and $\widehat{\mathbf{I}}_b$ are the spin operators of the two nuclei under study; v_a and v_b are the Larmor precession frequencies of the nuclei "a" and "b" at a field B_0; v_1 is the RF-field amplitude. Let us introduce the "center of the spectrum" frequency: $v_0 = \frac{v_a + v_b}{2}$ and the difference of Larmor frequencies $\delta v = v_a - v_b$. The off-set of the RF-frequency, v_{rf}, from the center of the spectrum is equal to $\Delta = v_0 - v_{rf}$. It is convenient to describe the spin dynamics in the frame of reference, which rotates about the v_{rf}-axis at the frequency v_{rf}. The Hamiltonian in such a rotating frame is as follows (when the counter-rotating RF-field component is disregarded):

$$\widehat{H}^{rf} = -\Delta_a \widehat{I}_{az} - \Delta_b \widehat{I}_{bz} - v_1(\widehat{I}_{ax} + \widehat{I}_{bx}) + J(\widehat{\mathbf{I}}_a \cdot \widehat{\mathbf{I}}_b) \quad (2)$$

Here $\Delta_a = v_a - v_{rf}$ and $\Delta_b = v_b - v_{rf}$ are the offsets of the RF-frequency from the resonance frequencies of spins "a" and "b",

respectively. Using the definitions Δ and δv we obtain: $\Delta_a = \Delta + \frac{\delta v}{2}$ and $\Delta_b = \Delta - \frac{\delta v}{2}$. Henceforth, in our analysis we assume that the RF-field strength, $v_1(t)$, is a function of time and search for the solution in the simplest case where $v_1(t)$ is changed in an adiabatic fashion. In this case it is sufficient to correlate the adiabatic levels of $\widehat{H}^{rf}$ at $v_1 = 0$ and at $v_1 \gg |J|, \delta v$. By correlation we mean that the population of the highest level (in energy) at $v_1 = 0$ goes to the population of the highest level at $v_1 \gg |J|, \delta v$; likewise, the population of the second highest state in the absence of the RF-field goes to the population of the second highest state in the presence of the RF-field and so on (here we assume that the energy levels do not cross, which is usually the case). Importantly, while performing the correlation of states we always stay in the RF-rotating reference frame (even when v_1 is zero) in order to remove all rapidly oscillating terms in the Hamiltonian.

2.2. Weakly coupled spins

The case of weakly coupled spins, $J \ll \delta v$, has been discussed in detail in previous papers [24–26]. Here we only briefly mention how state correlation should be performed.

The Hamiltonian (2) can be solved in the two limiting cases of $v_1 = 0$ and v_1 so strong that the effective precession frequencies of the two spins in the rotating frame, defined as $v_{a,b}^{eff} = \sqrt{v_1^2 + \Delta_{a,b}^2}$, differ only slightly. When $v_1 = 0$ the non-secular terms in the scalar product in Eq. (2) can be neglected and the eigen-states of $\widehat{H}^{rf}$ are $\{|\alpha\alpha\rangle = |T_+\rangle, |\beta\beta\rangle = |T_-\rangle, |\alpha\beta\rangle, |\beta\alpha\rangle\}$. The corresponding energies are as follows:

$$E(T_+) = -\Delta + \frac{J}{4}, \quad E(T_-) = \Delta + \frac{J}{4}, \quad E(\alpha\beta) = -\frac{\delta v}{2} - \frac{J}{4},$$
$$E(\beta\alpha) = \frac{\delta v}{2} - \frac{J}{4} \quad (3)$$

As usual, the spin-up and spin-down states are denoted as α and β, respectively. These states are grouped very differently depending on the value of Δ. Previously, it has been shown [24–26] that $|\Delta|$ should be chosen smaller than $\frac{1}{2}|\delta v|$. As a consequence, the second highest and second lowest states in energy are T_+ and T_-. The exact positions of the energy levels depend on the sign of Δ i.e. on v_{rf}.

At very strong v_1 so that $|v_a^{eff} - v_b^{eff}| \approx |\delta v_a^2 - \delta v_b^2|/v_1 \ll J$, the Hamiltonian is again simplified because the terms containing Δ_a and Δ_b can be neglected. In this situation one of the eigen-states is the singlet state, $|S\rangle$: when J is positive it is the second lowest state in energy, for negative J it is the second highest state. For simplicity (and without any loss of generality), here we always take $J > 0$ (for negative J the treatment can be done in a similar way). Thus, the second lowest state in energy has to be correlated with the S state at strong v_1, see Fig. 1a. By setting $0 < \Delta < \delta v$ this state becomes the T_+ state. Consequently, in both cases upon increasing the RF-field strength the singlet state should be correlated with the T_+ state. If we take $J < 0$ (or $\Delta < 0$) we will obtain $T_- \rightarrow S$ correlation. At thermal equilibrium, the T_+ state is overpopulated and the T_- state is underpopulated; thus, by state correlation upon increasing v_1 we can create an overpopulated or underpopulated singlet state and in this way generate triplet-singlet imbalance [28]. Owing to reversibility of adiabatic transitions, by decreasing v_1 from a high value (which guarantees that $|v_a^{eff} - v_b^{eff}| \ll J$) to zero we obtain $S \rightarrow T_+$ conversion (for positive Δ) or $S \rightarrow T_-$ conversion (for negative Δ). Thus, for the conversion pathway we can write down the following rule (here μ is either "+" or "−" and γ is gyromagnetic ratio):

$$S \leftrightarrow T_\mu, \quad \text{where} \quad \mu = \text{sgn}(J\gamma\Delta) \quad (4)$$
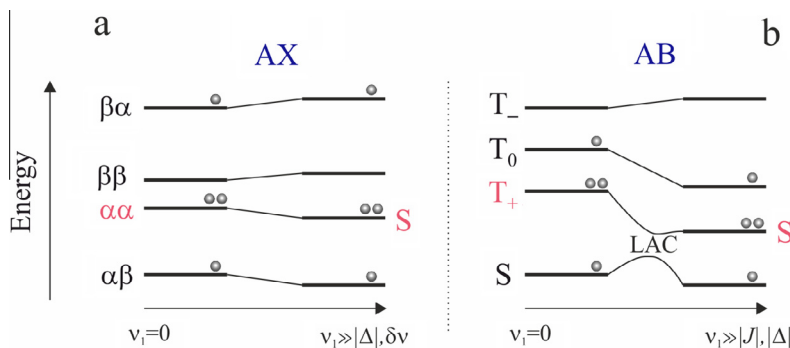
Fig. 1. Correlation of the adiabatic energy levels of (a) weakly-coupled AX two-spin system (i.e., $J \ll \delta v$) and (b) strongly coupled AB two-spin system (i.e., $J \gg \delta v$) in the reference frame rotating with v_0. In both cases at $v_1 = 0$ the second lowest state is the $\alpha\alpha = T_+$ state, which is correlated with the S state, being the second lowest at strong RF-field, $v_1 \gg J, \delta v$. The LAC in (b) is schematically indicated. Here $\Delta > 0, J > 0, v_a > v_b$; in (a) $\Delta < \delta v/2$, in (b) $\Delta < J$.

2.3. Strongly coupled spins

When the spin system is coupled strongly, it is convenient to present the Hamiltonian as a sum of the main part, $\widehat{H}_0$, and the perturbation, $\widehat{V}$,

$$\widehat{H}^{rf} = \widehat{H}_0 + \widehat{V},$$
$$\widehat{H}_0 = -\Delta(\widehat{I}_{az} + \widehat{I}_{bz}) - v_1(\widehat{I}_{ax} + \widehat{I}_{bx}) + J(\widehat{\mathbf{I}}_a \cdot \widehat{\mathbf{I}}_b), \quad \widehat{V} = -\delta v(\widehat{I}_{az} - \widehat{I}_{bz})/2$$

(5)

Here it is sufficient to correlate the states of only the main part, $\widehat{H}_0$. The perturbation $\widehat{V}$ repels the levels of $\widehat{H}_0$, when they tend to cross, see below. This situation is known as a Level Anti-Crossing (LAC). The solution of $\widehat{H}_0$ can be obtained for an arbitrary RF-field strength; when the RF-field is off $\widehat{H}_0$ has four eigenstates, $\{|S\rangle, |T_+\rangle, |T_0\rangle, |T_-\rangle\}$, with the following energies:

$$E(T_+) = -\Delta + \frac{J}{4}, \quad E(T_-) = \Delta + \frac{J}{4}, \quad E(T_0) = \frac{J}{4}, \quad E(S) = -\frac{3J}{4} \quad (6)$$

The order, in which the energy levels are grouped, is shown in Fig. 1b for the case $|J| > |\Delta|$ (also for $\Delta > 0, J > 0$). The lowest state is always the singlet state; the second lowest state is the T_+ state. When the RF-field is on and it is sufficiently strong, $v_1 \gg |\Delta|, |J|$, we obtain that the S state is second lowest for positive J, see Fig. 1b. One should note that APSOC only works when $|J| > |\Delta|$; otherwise the S state is the second lowest state at any v_1 value and singlet-triplet spin order conversion does not occur.

At thermal equilibrium the T_+ state is overpopulated; thus, this kind of conversion provides an overpopulated singlet state, thus, triplet-singlet imbalance is generated. It is also simple to show that by changing the sign of Δ (keeping its absolute value the same) the spin order conversion changes to $T_- \rightarrow S$ and the underpopulated T_- state produces the underpopulated S state, again, triplet-singlet imbalance is formed. Of course, upon decrease of v_1 we obtain $S \rightarrow T_+$ or $S \rightarrow T_-$ conversion.

As mentioned above, in a strongly coupled system, the role of the $\widehat{V}$ term is that it prevents from crossing of the states of $\widehat{H}_0$ and provides the desired correlation of the adiabatic states.

This is demonstrated, see Fig. 2, by calculating the energies of the eigen-states of the Hamiltonian $\widehat{H}^{rf}$. At $v_1 = 0$ the levels are grouped as also shown in Fig. 1b: the three triplet states are split by Δ and the S and T_0 states are split by J. As the RF-field increases, at a particular v_1 strength, namely, when $\sqrt{v_1^2 + \Delta^2}$ is equal to $|J|$, we obtain an S-T_+ (or S-T_-) crossing for the main Hamiltonian, $\widehat{H}_0$, see Fig. 2. In the absence of the perturbation there is no $S \leftrightarrow T_+$ or $S \leftrightarrow T_-$ conversion: instead the correlation of states is
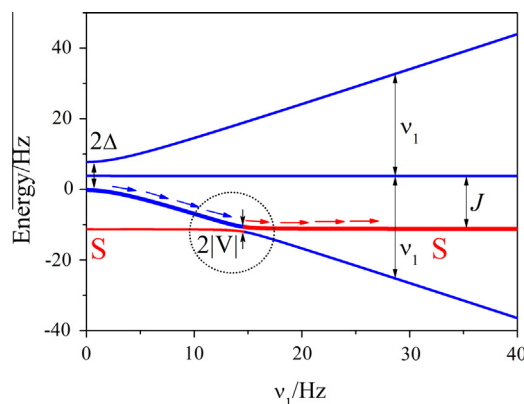
Fig. 2. Adiabatic correlation of states in the APSOC method for a strongly coupled spin system. Energy levels of the four spin states are shown as functions of v_1 for the following parameters: $J = 15$ Hz, $\Delta = 4$ Hz, $\delta v = 2$ Hz. In this example we have correlation of the T_+ state at $v_1 = 0$ with the singlet state, S, at $v_1 \gg J$; the corresponding adiabatic level, which is the second lowest level in energy, is highlighted and the spin order conversion pathway is indicated by arrows. This level has an LAC (indicated by the circle) with the lowest energy level; a prerequisite for the desired spin order conversion, $S \leftrightarrow T_+$, is adabatic passage through this LAC. The relevant splitting between the energy levels is indicated at $v_1 = 0$ and also at the LAC. When $\Delta < 0$ the energy level diagram looks the same except that the states T_+ and T_- at $v_1 = 0$ are exchanged and APSOC pathway becomes $S \leftrightarrow T_-$.

$S \leftrightarrow S$, i.e., the APSOC method does not work. So, the method works only because at the crossing we have the $\widehat{V}$ term, which mixes the crossing levels and makes an LAC out of the crossing. The time of passage through the crossing thus has to be of the order of $1/\delta v$ and does not have to be very precisely controlled (when the relaxation time is much greater than $1/\delta v$).

2.4. Intermediate coupling regime

Interestingly, our method also works for an arbitrary relation between J and δv. The reason for this is that at $v_1 = 0$ two of the spin eigen-states are always T_+ and T_- (the other two states are given by superposition of the states S and T_0) whereas at $v_1 \gg |J|, |\Delta|$ one of the eigen-states is the singlet state. In addition, it is possible to set the off-set Δ such that T_+ (or T_-) is the second lowest state in energy (in the RF-rotating frame) at $v_1 = 0$. Therefore, we can still perform conversion of the kind $S \leftrightarrow T_-$ or $S \leftrightarrow T_+$; when the relation between J and δv is arbitrary, the value of Δ should be set as follows for APSOC:

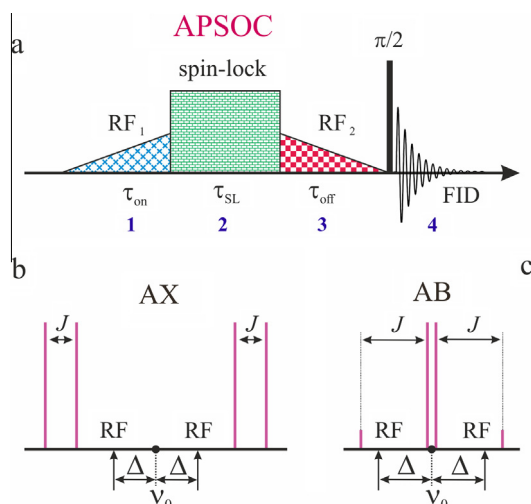$$|\Delta| < \frac{1}{2}\sqrt{\delta v^2 + J^2} + \frac{|J|}{2} \tag{7}$$

Thus, APSOC works for an arbitrarily coupled pair; its efficiency depends on how well the switching characteristics fulfills the requirement of adiabaticity and how well the M2S/S2M conversion time competes with relaxation. In order to facilitate the search for the optimal RF-field parameters for APSOC we developed software, which is available online [29]; examples of using this software are given in Appendix A. It is worth noting that when the sign of J is negative the conversion pathway changes as follows: it is $S \leftrightarrow T_-$ conversion (case $\Delta > 0$) and $S \leftrightarrow T_+$ conversion (case $\Delta < 0$). The reason is that at strong ν_1 the S state becomes the second highest state in energy. This change of the APSOC pathway is of no principal importance, since APSOC works essentially in the same way. In all cases, for the conversion pathway the rule (4) holds.

3. Experimental

3.1. Experimental protocol

To demonstrate the utility of the APSOC method we use the experimental protocol shown in Fig. 3. The protocol comprises four stages, see Fig. 3a: (M2S conversion)-(sustaining singlet order)-(S2M conversion)-(NMR detection). For the M2S/S2M conversion we exploit APSOC and set Δ in order to obtain spin order conversion of the kind $S \leftrightarrow T_-$ or $S \leftrightarrow T_+$. For sustaining the singlet order we use a spin-locking field in order to suppress singlet-triplet mixing. In Fig. 3b and c we also describe the appropriate way of setting the Δ value for weakly and strongly coupled spins.

An important point here is the performance of our method with respect to the M2S and S2M conversion efficiency. Assuming that relaxation during the spin-locking period equalizes the populations of the three triplet states but does not affect the singlet state, in APSOC we expect that after the two conversion stages the spin magnetization, M, equal to $\frac{2}{3}$ of the initial magnetization, M_0, remains. The $M = \frac{2}{3}M_0$ value obtained after the triplet relaxation has taken place is the theoretical upper limit for the M2S-S2M con-
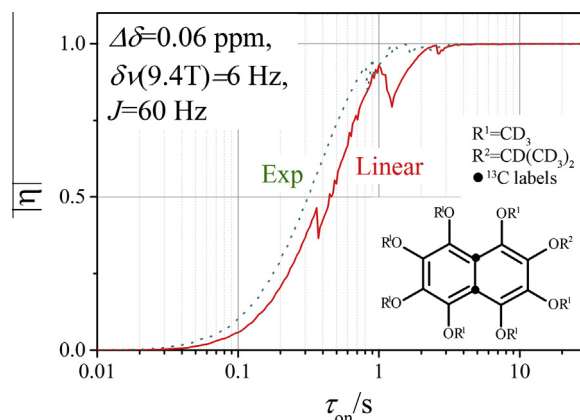
version efficiency [27], see Appendix B for details. Interestingly, when the duration of the APSOC experiment is smaller than all relaxation times in the spin system, the experimentally detected M can be even higher than $\frac{2}{3}M_0$ due to reversibility of adiabatic transitions (in the limiting case where the RF-excitation period is shorter than all relaxation times in the spin system $M = M_0$). Hereafter M/M_0 is denoted as ε; this parameter is used to indicate the signal left after APSOC.

As an example we evaluated the APSOC performance for a specific system of two nearly-equivalent ^{13}C spins in a naphthalene derivative, which are known to have an extraordinarily long LLS lifetime [6]. The results are shown in Fig. 4. It is readily seen that a smooth shaped pulse provides excellent $T_+ \rightarrow S$ conversion efficiency when the τ_{on} times are about 1 s or longer. Specifically, the absolute value of the η parameter (see Appendix A for explanation) is close to 1 indicating the high performance of APSOC. Thus, we anticipate that the APSOC method is useful for generating and observing LLSs in such a specifically designed molecule with nearly equivalent spins.

Additionally, we made a comparison of APSOC and the so-called Spin-Locking Induced Crossing (SLIC) method [30], which is a technique for generating LLS in pairs of nearly equivalent spins. Details of the SLIC method are given in Appendix C. In the SLIC method, see explanation below, the system is brought to the same LAC as discussed above, see Fig. 2, but in a non-adiabatic way with the $\hat{V}$ term driving the singlet-triplet transitions.

3.2. Sample preparation

Experiments were performed for aqueous solutions of a dipeptide, H-Cys-Gly-OH (hereafter, Cys-Gly), at a 700 MHz NMR spectrometer. LLSs are created for the strongly coupled α-CH$_2$ protons of the Gly-residue ($J = 17.2$ Hz, $\delta\nu = 15.5$ Hz at 700 MHz) and the weakly coupled β-CH$_2$ protons of the Cys-residue ($J = 12.4$ Hz, $\delta\nu = 145$ Hz at 700 MHz). The sample contains 30 mM of Cys-Gly (Bachem, G-3755) and 10 mM of EDTA at pH 12.0 in D$_2$O. The sample was bubbled by N$_2$ for 10 min to remove the dissolved oxygen. EDTA was used to chelate with paramagnetic ions.

Fig. 3. Experimental protocol used for generating, sustaining and observing LLSs (a). In stage **1** magnetization is converted into the singlet state (by APSOC we perform conversion of the kind $T_+ \rightarrow S$ or $T_- \rightarrow S$) by the RF$_1$-field, which is adiabatically turned on during the time period τ_{on}. In stage **2** the singlet state is sustained during a variable time interval τ_{SL} (by using spin locking, or without spin-locking when $J \gg \delta\nu$). In stage **3** the singlet state is converted back into z-magnetization by the RF$_2$-field, which is adiabatically turned off during the time period τ_{off}. Finally, in stage **4** the NMR spectrum is taken by using a $\pi/2$-pulse. The frequency of the RF$_1$- and RF$_2$-fields is equal to ($\nu_0 \pm \Delta$). In (b) and (c) we present the appropriate choice of Δ for the desired $T_+ \leftrightarrow S$ and $T_- \leftrightarrow S$ conversion for a weakly coupled (AX) and strongly coupled (AB) spin system, respectively.

Fig. 4. Calculated dependence of the APSOC efficiency $|\eta|$ on the τ_{on} time of RF-field switching. η is measured as described by Eq. (A6) and characterizes the efficiency of singlet order formation: $|\eta| = 1$ stands for complete conversion and $\eta = 0$ means that no triplet-singlet imbalance is generated. The calculation is done without taking into account relaxation processes and considers two ^{13}C nuclei of a naphthalene derivative that are indicated by black dots in the Figure. The ^{13}C spin pair has a long-lived state with a lifetime of ~1 h [1]. Parameters of the spin system: chemical shift difference is 0.06 ppm, $\delta\nu(9.4T) = 6$ Hz, $J = 60$ Hz, $\Delta = 10$ Hz. Parameters of the RF-field profile (ν_1^{max} and k values) are optimized; calculations are performed for linear (solid line) and exponential (dashed line) profiles of RF-field switching.
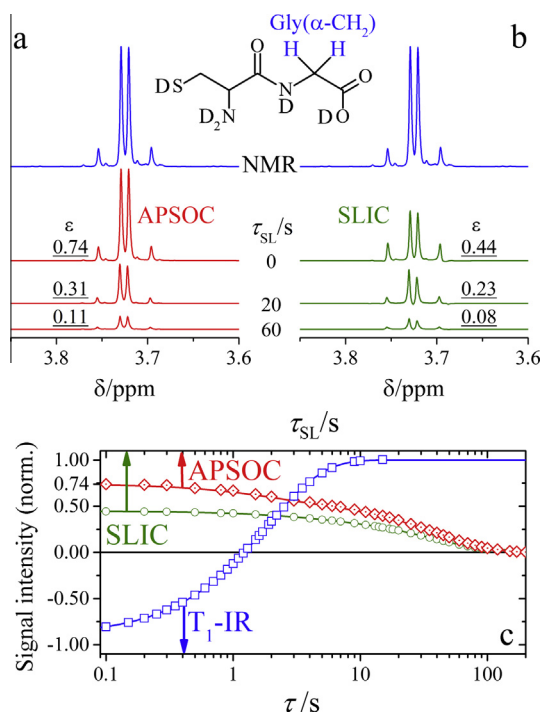
Fig. 5. (a) and (b) 700 MHz ^1H NMR spectra of Gly(α-CH$_2$) protons of Cys-Gly with APSOC and SLIC spectra for different duration, τ_{SL}, of the spin-locking stage. Signal intensities, ε, are shown at the spectra (underlined numbers). (c) τ_{SL} time dependence of the NMR intensity of the α-CH$_2$ protons. The signal intensity is given in units of the thermal polarization, indicating that after APSOC we obtain about 3/4 of the starting spin magnetization and in SLIC less than 1/2. The τ_{SL} dependences are fitted by the function $\varepsilon(\tau_{SL}) = A_T \times \exp(-\tau_{SL}/T_T) + A_S \times \exp(-\tau_{SL}/T_S)$; the fitting parameters for APSOC are: $T_T = 1.73$ s, $T_S = 39.8$ s, $A_T = 0.17$, $A_S = 0.57$ and for SLIC: $T_T = 2.9$ s, $T_S = 39.6$ s, $A_T = 0.055$, $A_S = 0.385$. Experimental APSOC parameters are: $\tau_{on} = \tau_{off} = 0.4$ s, $\upsilon_1^{max} = 70$ Hz, $\upsilon_{SL} = 1$ kHz, τ_{SL} is varied, $\upsilon_0 = 3.726$ ppm, $\Delta = 12$ Hz. Experimental SLIC parameters are: $\tau_{SLIC} = 45.46$ ms, $\upsilon_{SLIC} = 17.5$ Hz, $\upsilon_{SL} = 1$ kHz, τ_{SL} is varied, $\upsilon_0 = 3.726$ ppm. In (c) we also show the result of the conventional inversion-recovery experiment (dependence of the NMR signal on the recovery time, τ) used for T$_1$-measurements providing $T_1 = 1.9$ s.

4. Results and discussion

Typical NMR spectra obtained using the APSOC method are shown in Fig. 5a for different sustaining times, τ_{SL}: at long τ_{SL} of about 60 s the NMR signals are still visible, clearly indicating the presence of an LLS. The full τ_{SL} dependence, see Fig. 5c, allowed us to find the singlet order lifetime T_S, which equals $21 \cdot T_1$ at 700 MHz. Thus, we indeed create an LLS, i.e., singlet order, in the spin pair under study. As far as the performance of our spin order conversion method is concerned, one can clearly see that after the M2S-S2M conversion the NMR signal remains strong as compared to the initial thermal signal M_0. Namely, the signal is $0.74 \cdot M_0$ at short τ_{SL} and goes to $\frac{M_0}{3}$ at $\tau_{SL} \approx 20$ s, i.e., at spin-locking times, which are much longer than T_1. When the τ_{SL}-dependence is approximated by a sum of two exponential functions, $M(\tau_{SL}) = A_T \exp(-\tau_{SL}/T_T) + A_S \exp(-\tau_{SL}/T_S)$ (fast and slow exponent, $T_T < T_1$), the weight of the slow component, A_S, is about $0.57 \cdot M_0$. Thus, our method indeed provides excellent M2S-S2M conversion efficiency. Here we attribute the loss of the slow component at $\tau_{SL} \to 0$ to relaxation during the RF-on/RF-off periods. In general, when it becomes possible to reduce the RF-switching time so that $(\tau_{on} + \tau_{off}) \ll T_1$ (in our example, $\tau_{on} + \tau_{off} \approx T_1/3$) we expect that the weight of the slow component reaches $\frac{2}{3}M_0$. We would like to stress that ε can be higher than 2/3, reaching unity for perfectly adiabatic RF-field variation in the absence of spin relaxation (because the RF-on switch and subsequent RF-off switch

bring the spin system back to its initial state with $M = M_0$). At the same time, the amplitude of the slow component, which corresponds to the singlet spin order, in the $M(\tau_{SL})$ dependence cannot be greater than $\frac{2}{3}M_0$. Our experimental results are consistent with these considerations.

Additionally, we performed SLIC experiments for the same spin pair as described in Appendix C, which provide a similar τ_{SL} dependence; however, the conversion efficiency in the SLIC case is systematically lower, see Fig. 5b. For instance, at short τ_{SL} we obtain $M < \frac{M_0}{2}$ in the SLIC case. One should also note that after application of SLIC the NMR spectral pattern is distorted (specifically, the intensity ratio for the central and outer components is not the same as in the thermal spectrum) in contrast to that obtained after APSOC. In principle, robustness of the SLIC method can be improved [31] by using composite and shaped pulses; the latter method is similar to APSOC. The difference between the two methods is that in APSOC we are converting the longitudinal magnetization to the singlet order, whereas in SLIC with shaped pulses transverse magnetization is used.

Additionally, we studied the influence of the spin-locking field on the singlet sustaining efficiency. When $J \sim \delta\upsilon$ spin-locking makes the LLS lifetime longer: T_S increases from 6 s to 40 s for the Gly(α-CH$_2$) protons, see Appendix D. This finding is in agreement with the results of DeVience et al. [32] who investigated the T_S dependence on the spin-locking field strength.

As mentioned above, our method works for both weakly and strongly coupled spin pairs. In this work, the APSOC method was also applied to the weakly-coupled β-CH$_2$ protons of the Cys residue, see Fig. 6. At $\tau_{SL} \to 0$ we obtain $M = 0.72 \cdot M_0$; the τ_{SL} dependence shows that we clearly generate an LLS ($T_S = 5.8$ s, which is about $4.8 \cdot T_1$). The SLIC method is not directly applicable to this
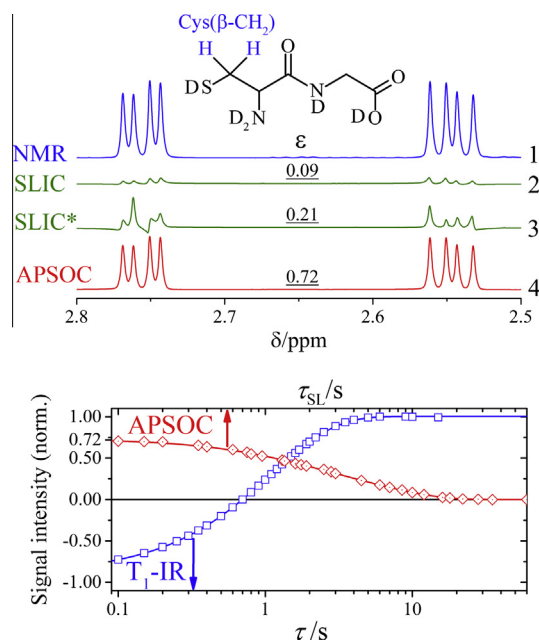
Fig. 6. (Top) 700 MHz ^1H NMR spectrum of the Cys(β-CH$_2$) protons of Cys-Gly (trace 1); SLIC spectrum obtained with parameters $\tau_{SLIC} = 4.8$ ms, $\upsilon_{SLIC} = 12.7$ Hz, $\tau_{SL} = 0$, $\upsilon_0 = 2.651$ ppm (trace 2); optimized SLIC* spectrum obtained with parameters $\upsilon_{SLIC} = 37$ Hz, $\tau_{SL} = 100$ ms and $\upsilon_0 = 2.651$ ppm (trace 3); APSOC spectrum obtained with parameters: $\tau_{on} = \tau_{off} = 0.2$ s, $\upsilon_1^{max} = 550$ Hz, $\upsilon_{SL} = 1$ kHz, $\tau_{SL} = 0$, $\upsilon_0 = 2.651$ ppm (trace 4). Signal intensities, ε, given in units of thermal spin magnetization, are shown in the spectra by underlined numbers. (bottom) τ_{SL} dependence of the NMR intensity of Cys(β-CH$_2$) protons in the APSOC experiment. After APSOC at $\tau_{SL} = 0$ we obtain $\varepsilon \approx 0.72$; the τ_{SL} dependences are fitted by function $\varepsilon(\tau_{SL}) = A_T \times \exp(-\tau_{SL}/T_T) + A_S \times \exp(-\tau_{SL}/T_S)$; the fitting parameters are: $T_T = 1.2$ s, $T_S = 5.8$ s, $A_T = 0.2$, $A_S = 0.52$; results of the inversion-recovery experiment are also shown.

system, because, literally, there is no LAC at $v_1 \approx |J|$ in this case. After an optimization the SLIC method can be nonetheless used, but its performance is much lower than for APSOC, see Fig. 6 and Appendix C. This allows us to conclude that SLIC is an efficient but limited method, designed specifically for strongly-coupled spin pairs, i.e., $J > \delta v$ or even $J \gg \delta v$.

An important issue for our method is the setting of the τ_{on} and τ_{off} times and the maximal v_1-value of the switched RF-fields such that $\xi_{ij}(t) \ll 1$ during the switch to guarantee adiabaticity. Here we do not optimize the exact $v_1(t)$ time profile and only vary the maximal RF-field strength v_1^{max} and the switching time τ_{on} (or τ_{off}) by running numerical calculations. Examples of such optimization are shown in Appendix A. Once τ_{on} and τ_{off} are above a certain threshold value (minimal time compatible with adiabatic variation of the Hamiltonian) there is no benefit to increase them further, since spin relaxation during the pulses reduces the spin order. The Δ parameter can be set according to Eq. (7). One should also note that the RF-field switches between stages 1 (turning on the RF-field), 2 (sustaining the singlet state by spin-locking), 3 (turning off the RF-field), see Fig. 3, result in non-adiabatic changes of the spin Hamiltonian. However, these switches do not affect the singlet state population (because the singlet is nearly an eigen-state of the Hamiltonian in all cases) and do not disturb the singlet spin order.

5. Conclusions

In summary, a general method for generating and observing singlet spin order is proposed, which works for strongly coupled spin pairs as well as for weakly coupled spin pairs. The technique is simple in use and requires setting only the frequency of the switched RF-field together with the ramp of RF-field switching. The switched RF-field thus works as an NMR "pulse", which induces spin order conversion of the kind $S \leftrightarrow T_+$ or $S \leftrightarrow T_-$. Furthermore, by varying the frequency of the switched RF-fields, one can change the "phase" of the APSOC "pulses" and arrange a pseudo "phase cycle" [24]. As will be shown in a separate publication, such a procedure suppresses residual background signals, leaving only the signals of spin pairs under investigation. This makes our method very useful for selecting signals of a particular spin pair and for analyzing LLSs in a situation where the NMR spectrum is crowded. Thus, our general method for generating and observing singlet spin order creates a new powerful resource for studying LLSs in macromolecules such as proteins and RNA/DNA fragments.

We anticipate that our method is useful in many other situations as well. For instance, it can be applied to systems with more than two spins, e.g., to three-spin systems [24]. APSOC can be a method of choice to generate and observe LLSs in pairs of nearly equivalent spins, which are found in low-field experiments [7,33] and specially designed molecules [6,12,13,18], see Fig. 4. In fact the method works efficiently not only for pairs of chemically inequivalent spins but also for cases of chemical equivalence but magnetic inequivalence of spins induced via J-couplings to additional spins. Interestingly, the final part of the APSOC sequence (stage 3) has already been applied [34] to an AA′MM′-spin system to transfer singlet spin order of the AA′-spins to their $T_\pm$ - state. This is of importance for pumping "disconnected" eigen-states in magnetic resonance [31,35].

The ease of our method, the possibility of using APSOC for spin pairs with an arbitrary relation between J and δv is highly promising for generating and observing LLSs. One more topical application is preserving and manipulating spin hyperpolarization [16–19]. In particular, our method can be used in para-Hydrogen Induced Polarization (PHIP) experiments [36,37]: when PHIP is generated

in a pair of strongly coupled protons (e.g., at low magnetic fields) there is a need to convert the spin order into observable spin magnetization. APSOC perfectly fits to this experimental need. Likewise, it is compatible with other hyperpolarization methods notably, with dynamic nuclear polarization: presently, the most general hyperpolarization technique. APSOC can be used to overcome the severe limitation imposed by T_1-relaxation, which is a stumbling block for many applications of hyperpolarization in NMR spectroscopy and imaging. Last but not least, our method can be used to generate "entangled" quantum states, which are in the heart of quantum computing and quantum information processing [38,39].

Appendix A. APSOC performance and optimization

To find out what the conditions are for adiabatic RF-field switches in APSOC we have performed numerical calculations of the singlet order conversion efficiency.

The thermal density matrix of a two spin-system is as follows:

$$\hat{\rho}_0 = \frac{\hat{E}}{4} + \zeta(\hat{I}_{az} + \hat{I}_{bz}) = \frac{\hat{E}}{4} + \zeta(\hat{\rho}_{T_+} - \hat{\rho}_{T_-}) \tag{A1}$$

Here ζ is the Boltzmann factor, $\hat{I}_{1z}$ and $\hat{I}_{2z}$ are the z-projections of spins "a" and "b"; consequently the matrices $\xi\hat{\rho}_{T_+}$ and $\xi\hat{\rho}_{T_-}$ account for the equilibrium populations of the T_+ and T_- states. We also introduce the density matrix of the S state, $\hat{\rho}_S$. When necessary, the matrices $\hat{\rho}_S$, $\hat{\rho}_{T_-}$ and $\hat{\rho}_{T_+}$ can be written in the spin-operator form:

$$\hat{\rho}_{T_+} = |T_+\rangle\langle T_+| = \frac{\hat{E}}{4} + \frac{\hat{I}_{az}}{2} + \frac{\hat{I}_{bz}}{2} + \hat{I}_{az}\hat{I}_{bz} \tag{A2a}$$

$$\hat{\rho}_{T_-} = |T_-\rangle\langle T_-| = \frac{\hat{E}}{4} - \frac{\hat{I}_{az}}{2} - \frac{\hat{I}_{bz}}{2} + \hat{I}_{az}\hat{I}_{bz} \tag{A2b}$$

$$\hat{\rho}_S = |S\rangle\langle S| = \frac{\hat{E}}{4} - (\hat{\mathbf{I}}_a \cdot \hat{\mathbf{I}}_b) \tag{A2c}$$

In APSOC transfer of population of the T_+ or T_- states into population of the S state (and vice versa) occurs, depending on the RF-frequency. When we apply the adiabatic $T_+ \to S$ and $T_- \to S$ pulses, the density matrix changes as follows:

$$\hat{\rho}_0 \overset{T_+ \to S}{\to} \frac{\hat{E}}{4} + \zeta(\hat{\rho}_S + \hat{\rho}'_+) \tag{A3a}$$

$$\hat{\rho}_0 \overset{T_- \to S}{\to} \frac{\hat{E}}{4} - \zeta(\hat{\rho}_S + \hat{\rho}'_-) \tag{A3b}$$

Here the density matrices $\hat{\rho}_+$ and $\hat{\rho}_-$ stand for the residual triplet spin order; both matrices are "orthogonal" to $\hat{\rho}_S$: $\text{Tr}\{\hat{\rho}_+\hat{\rho}_S\} = \text{Tr}\{\hat{\rho}_-\hat{\rho}_S\} = 0$. From Eqs. (A3) we compute the following singlet-state population, n_S:

$$n_S = \frac{1}{4} + \zeta, \quad \text{for } T_+ \to S \tag{A4a}$$

$$n_S = \frac{1}{4} - \zeta, \quad \text{for } T_- \to S \tag{A4b}$$

In the general case, i.e., when adiabaticity is not perfectly fulfilled, the resulting density matrix differs from Eq. (A3). In such a situation the simple relations (A3) do not hold and the final density

matrix is equal to $\hat{\rho}_{fin} = \hat{\hat{Q}} \hat{\rho}_0$, where $\hat{\hat{Q}}$ is the super-operator describing the spin evolution; the resulting singlet-state population is equal to

$$n_S = \text{Tr}\{\hat{\rho}_S \cdot \hat{\hat{Q}} \hat{\rho}_0\} = \frac{1}{4} + \zeta \cdot \text{Tr}\left\{\hat{\rho}_S \cdot \hat{\hat{Q}} [\hat{\rho}_{T_+} - \hat{\rho}_{T_-}]\right\} \quad (A5)$$

To make a quantitative account for imperfect adiabaticity we introduce the following parameter, which characterizes the singlet order conversion efficiency:

$$\eta = \frac{n_S - \frac{1}{4}}{\zeta} = \text{Tr}\{\hat{\rho}_S \cdot \hat{\hat{Q}} [\hat{\rho}_{T_+} - \hat{\rho}_{T_-}]\} \quad (A6)$$

Thus η is the measure of singlet order conversion efficiency for an arbitratry M2S conversion method. The η parameter changes in the range from -1 to $+1$. Specifically, for population transfer between the T_- and S states we obtain $\eta = -1$, while for the $T_+ \to S$ conversion we obtain $\eta = +1$; when $\eta = 0$ the singlet state is neither overpopulated nor underpopulated, i.e., $n_S = \frac{1}{4}$. Hence the absolute value of the η parameter should be maximized in order to find the optimal conditions for the M2S/S2M conversion. Here we performed optimization only for the M2S conversion because in the case of adiabatic transitions the S2M conversion proceeds in the same way. For the sake of simplicity, here we did not consider spin relaxation. In a simple way, the relaxation effects can be taken into account by optimizing the RF-switching profile under the constraint that the τ_{on} time is shorter than the relaxation times of the spin system.

We investigated how the absolute value of the η parameter changes upon variation of the J and δv parameters, as well as the switching time, τ_{on}, and the switching profile.

In Fig. A1 we show the optimal APSOC efficiency for a pair of protons as a function of τ_{on}. In the calculation we used linear and exponential profiles (the results for other profiles can be obtained and analyzed in the same way), which are optimized: for the linear profile the v_1^{max} value is optimized, for the exponential profile two parameters, v_1^{max} and k (characterizing the ramp of the RF-on field), are optimized. It is clearly seen that at long τ_{on} times the APSOC efficiency approaches unity, whereas at short τ_{on} it is zero because the conditions for adiabatic variation of the Hamiltonian are not fulfilled. At $\delta v \gg J$, i.e., for a weakly-coupled spin system the time compatible with adiabatic variation of the Hamiltonian is given by $1/J$. In the opposite case, $\delta v \ll J$, of a strongly-coupled spin system the switching time compatible with adiabatic variation of the Hamiltonian is given by $1/\delta v$. "Adiabatic variation" implies that the Hamiltonian is varied slowly; however, one can see that the τ_{on} times providing the APSOC efficiency of already 0.5 are not that long: they are of the order of $1/J$ (in a weakly-coupled spin pair) or $1/\delta v$ (in a strongly-coupled spin pair).

Appendix B. M2S/S2M conversion efficiency in APSOC

Let us derive here the magnetization value after two M2S/S2M conversion stages.

For spins having small thermal polarization we obtain the following populations of the spin states (here a strongly-coupled spin pair is considered as an example):

$$n_{T_+} = \frac{1}{4}(1 + P), \quad n_{T_-} = \frac{1}{4}(1 - P), \quad n_{T_0} = n_S = \frac{1}{4} \quad (B1)$$

Hence the net spin magnetization is equal to $M_0 = n_{T_+} - n_{T_-} = \frac{P}{2}$. Here $P = 4\zeta$ stands for the population differences between the spin states at equilibrium conditions. Let us assume that spin relaxation during the M2S/S2M conversion step is negligible and assume that we have $S \leftrightarrow T_+$ conversion (the results for $S \leftrightarrow T_-$ conversion are exactly the same). In this situation after the M2S conversion the
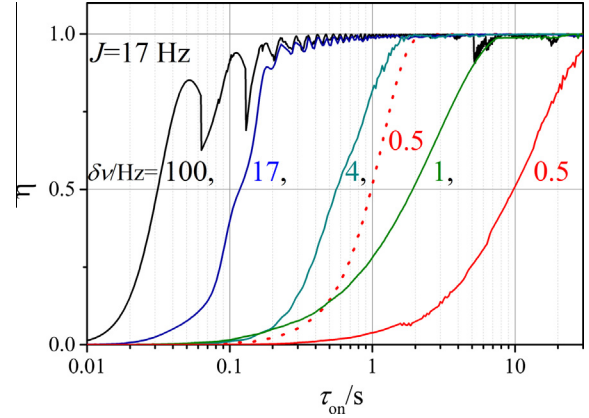
Fig. A1. Calculated dependence of $|\eta|$ on the τ_{on} time of RF-field switching. The APSOC efficiency is measured as described by Eq. (A6). The calculation is done without taking relaxation processes into account. Here $J = 17$ Hz, $\Delta = 10$ Hz, δv is varied. The RF-field switching on profiles are linear $v_1(t) = v_1^{max}(t/\tau_{on})$ (solid lines) or exponential $v_1(t) = v_1^{max} \frac{1-\exp(-kt)}{1-\exp(-k\tau_{on})}$ (dotted line); here $0 < t < \tau_{on}$. The parameters of the field profile (the v_1^{max} value for the linear profile; the v_1^{max} value and k for the exponential profile) are optimized to obtain the maximal APSOC efficiency for the given spin-system and τ_{on} and Δ parameters.

population of the S-state is equal to $\frac{1}{4}(1 + P)$. When the singlet sustaining time, τ_{SL}, is longer than the T_1 -relaxation time but shorter than T_S the populations of the three triplet states are rapidly equalized and become equal to $n_T = \frac{1}{4} - \frac{P}{12}$. After the S2M conversion step the state populations are

$$n_{T_+} = \frac{1}{4}(1 + P) \quad , n_{T_-} = n_{T_0} = n_S = n_T = \frac{1}{4} - \frac{P}{12} \quad (B2)$$

Consequently, the spin magnetization becomes

$$M = n_{T_+} - n_{T_-} = \frac{P}{3} = \frac{2}{3}M_0 \quad (B3)$$

Thus, $\frac{1}{3}$ of the initial magnetization is irreversibly lost. Previously it has been shown [22] that such losses are inevitable, i.e., the M2S-S2M conversion efficiency is smaller than 1. When $\tau_{SL} \ll T_1, T_S$ we obtain $M = M_0$ because adiabatic transitions are reversible: the RF$_1$-field redistributes the spin state populations but the RF$_2$-field returns them back to the initial values.

When spin relaxation during the switches comes into play it reduces the resulting M value because during the switch the singlet state is not an eigen-state of the Hamiltonian, with the consequence that all spin states are affected by T_1- and T_2-relaxation. This results in the loss of singlet spin order, i.e., in a reduction of the measured M value.

Appendix C. Comparison of APSOC and SLIC

Above we argue that APSOC, as a more general method, is advantageous as compared to the SLIC technique. Here we present further detail of this comparison.

SLIC is dealing with spin order conversion in strongly-coupled spin pairs [26]. The SLIC protocol is presented in Fig. C1. In this protocol, first the transverse y -magnetization is formed by a $\left(\frac{\pi}{2}\right)_x$ -pulse. Then an RF-field is applied during a time period τ_{SLIC} along the y-axis of the rotating frame. The RF-frequency should be equal to v_0, see Fig. C1a. When the RF-field amplitude matches the J value, it induces M2S transitions, i.e., coherent spin order conversion driven by δv. After τ_{SLIC} equal to half-period of the coherent evolution the conversion efficiency is maximal. After that singlet spin order is preserved during time interval τ_{SL} by
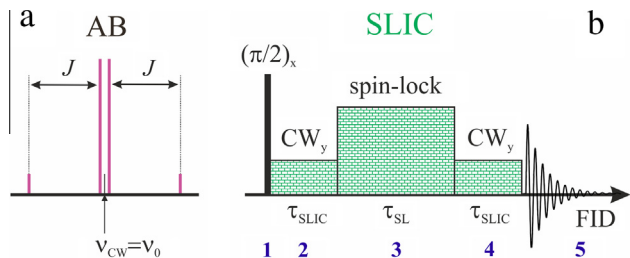
Fig. C1. (a) Setting of the RF-frequency for SLIC and (b) experimental protocol used in the SLIC method. The protocol shown in (b) comprises 5 stages. In stage **1** transverse magnetization is formed by a $\left(\frac{\pi}{2}\right)_x$ -pulse; then, in stage **2**, the magnetization is converted into singlet order by the RF-field, which has the y-phase, amplitude $v_1 = |J|$ and duration of $\tau_{SLIC} = 1/\sqrt{2}\delta v$. In stage **3**, the singlet state is sustained during a variable time interval τ_{SL} (by using spin locking with $v_1 \gg J, \delta v$ or in the absence of spin-locking when $J \gg \delta v$). In stage **4** the singlet state is converted back into y-magnetization by the RF-field, which has the y-phase, amplitude $v_1 = |J|$ and duration of $\tau_{SLIC} = 1/\sqrt{2}\delta v$. Finally, in stage **5** the NMR spectrum is taken.

introducing spin-locking by a strong RF-field (its amplitude does not match J in order to prevent from spin order conversion). Finally, with the aim to observe the singlet state, the singlet spin order is converted back into transverse magnetization by an RF-field applied during a time period τ_{SLIC} along the y-axis of the rotating frame (again, the RF-amplitude matches the J value).

First, we evaluated the spin order conversion efficiency in APSOC and in SLIC by numerical calculations, see Fig. C2. For a strongly-coupled spin system both techniques work well; as far as the time required for spin order conversion is concerned, SLIC provides faster conversion. At the same time, SLIC requires precise setting of the mixing time τ_{SLIC}, whereas in APSOC it is sufficient that τ_{on} exceeds a certain threshold value. When the spin system is coupled weakly, the SLIC method does not work well anymore. This situation is, in principle, beyond the range of applicability of the method, since there is no crossing at $v_1 = |J|$ in a weakly-coupled spin system. However, SLIC can still perform the M2S transfer but (i) its efficiency becomes low and (ii) the τ_{SLIC} dependence contains fast oscillations, so that the transfer process can be difficult to control. At the same time, APSOC works perfectly in both cases.

In Fig. 5 the performance of the two techniques is compared for the strongly coupled spin pair of the Gly-residue in the dipeptide. It is clearly seen that both methods perform the conversion and sustain the LLS (NMR signals are visible after 60 s of spin-locking), but APSOC always provides higher NMR signal intensities. This is demonstrated by the τ_{SL} dependence, see Fig. 5c: in SLIC and APSOC the signals decay at the same rate but in APSOC the signals are always stronger. When $\tau_{SL} \rightarrow 0$ after the M2S-S2M conversion efficiency $\varepsilon = 0.72$ of the initial thermal magnetization remains, whereas for SLIC it is below 0.5. By fitting the τ_{SL} dependence obtained with APSOC as a sum of two exponents (the slow component stands for the LLS) we found $A_S = 0.52$, i.e., a strong contribution from the singlet spin order. In a weakly-coupled spin pair (Cys-residue) the performance of APSOC is the same as in the previous case whereas the performance of SLIC is strongly reduced (as expected), see Fig. 6.

Appendix D. Sustaining singlet order

In our experiments, in order to sustain the long-lived singlet order we use spin locking. The idea behind it is that in the presence of a strong RF-field the singlet state is a true eigen-state of a spin pair. This is a valid assumption once the difference, δv_{eff}, of the precession frequencies of the spins (in the rotating frame) becomes smaller than J:
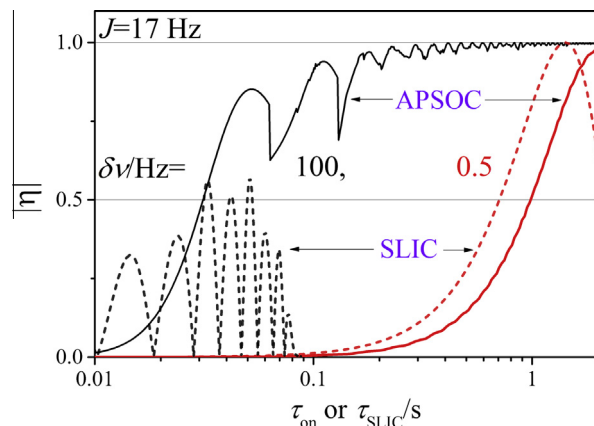
Fig. C2. Calculation of the relative performance for the M2S conversion efficiency: dependence of singlet-state population of τ_{on} for APSOC (solid lines) and dependence of the singlet state population on τ_{SLIC} for SLIC (dashed lines). The APSOC efficiency is measured as described by Eq. (A6). The calculation is done without taking into account relaxation processes. Here $J = 17$ Hz, $\Delta = 10$ Hz, δv is 100 Hz (black lines) or 0.5 Hz (red lines). In APSOC the RF-field switching-on profiles are linear. The parameters of the field profile (the v_1^{max} value) are optimized to obtain the maximal APSOC efficiency for the given spin-system and τ_{on} and Δ parameters. (For interpretation of the references to colour in this figure legend, the reader is referred to the web version of this article.)
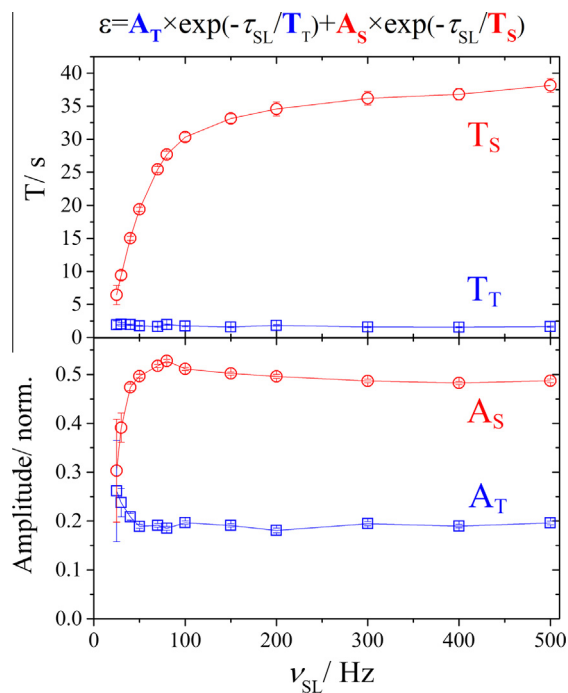
Fig. D1. Dependence of the singlet order sustaining efficiency on the amplitude of the spin-locking RF-field, v_{SL}, for the lifetimes of the fast, T_T, and slow, T_S, components (top) and the weights of these components (bottom) obtained for the α-CH$_2$ protons of the Gly-residue of Cys-Gly. Experimental parameters are: $\tau_{on} = \tau_{off} = 0.4$ s, $v_1^{max} = 70$ Hz, $v_0 = 3.726$ ppm, $\Delta = 12$ Hz, $B_0 = 16.4$ T; a linear field switching profile is used. To obtain the sustaining efficiency we fitted the $\varepsilon(\tau_{SL})$ dependence by a bi-exponential function. As above, ε is the spin magnetization obtained in the APSOC experiment measured in units of the thermal magnetization.

$$|\delta v_{eff}| \ll |J| \tag{D1}$$

Let us consider this condition in further detail. In the rotating frame the spins precess at the following frequencies:

$$v_a^{eff} = \sqrt{\Delta_a^2 + v_1^2}; \quad v_b^{eff} = \sqrt{\Delta_b^2 + v_1^2} \tag{D2}$$

When $v_1 \gg |\Delta_a|, |\Delta_b|$ we obtain that $\delta v_{eff} \to 0$, i.e., the singlet state is indeed sustained by the RF-field.

A specific case is given by a strongly coupled pair: in such a pair the singlet state is in good approximation an eigen-state with the consequence that it is sustained even without spin-locking, for example, see Ref. [1]. In the example presented here, the Cys-Gly peptide, sustaining the LLS in the absence of spin-locking is rather inefficient even for the CH_2-protons of Gly ("strongly-coupled" spin pair) because the absolute values of J and δv are similar, i.e., the condition $|J| \gg |\delta v|$ does not hold. To analyze the effect of the spin-locking RF-field we analyzed the τ_{SL}-dependence of NMR signals in APSOC at variable v_{SL}. The time dependence was fitted by a biexponential function: the fast component was attributed to triplet relaxation with a characteristic time T_T while the slow component was attributed to the LLS. The results are given in Fig. D1: the T_S time is relatively short in the absence of spin-locking and strongly increases upon increase of v_{SL}. At the same time, the weight of the slow component increases, demonstrating that spin-locking indeed prolongs the LLS lifetime.

References

[1] M.H. Levitt, Singlet nuclear magnetic resonance, in: M.A. Johnson, T.J. Martinez (Eds.), Annual Review of Physical Chemistry, Annual Reviews, Palo Alto, 2012, pp. 89–105.

[2] G. Pileio, Relaxation theory of nuclear singlet states in two spin-1/2 systems, Prog. NMR Spectrosc. 56 (2010) 217–231.

[3] A.S. Kiryutin, S.E. Korchak, K.L. Ivanov, A.V. Yurkovskaya, H.-M. Vieth, Creating long-lived spin states at variable magnetic field by means of photo-chemically induced dynamic nuclear polarization, J. Phys. Chem. Lett. 3 (2012) 1814–1819.

[4] A.N. Pravdivtsev, A.V. Yurkovskaya, H. Zimmermann, H.-M. Vieth, K.L. Ivanov, Magnetic field dependent long-lived spin states in amino acids and dipeptides, Phys. Chem. Chem. Phys. 16 (2014) 7584–7594.

[5] G. Pileio, M. Carravetta, E. Hughes, M.H. Levitt, The long-lived nuclear singlet state of ^{15}N-nitrous oxide in solution, J. Am. Chem. Soc. 129 (2008) 12582–12583.

[6] G. Stevanato, J.T. Hill-Cousins, P. Håkansson, S.S. Roy, L.J. Brown, R.C.D. Brown, G. Pileio, M.H. Levitt, A nuclear singlet lifetime of more than one hour in room-temperature solution, Angew. Chem. Int. Ed. 54 (2015) 3740–3743.

[7] M. Carravetta, O.G. Johannessen, M.H. Levitt, Beyond the T_1 limit: singlet nuclear spin states in low magnetic fields, Phys. Rev. Lett. 92 (2004) 153003.

[8] A. Bornet, P. Ahuja, R. Sarkar, L. Fernandes, S. Hadji, S.Y. Lee, A. Haririnia, D. Fushman, G. Bodenhausen, P.R. Vasos, Long-lived states to monitor protein unfolding by proton NMR, ChemPhysChem 12 (2011) 2729–2734.

[9] R. Sarkar, P.R. Vasos, G. Bodenhausen, Singlet-state exchange NMR spectroscopy for the study of very slow dynamic processes, J. Am. Chem. Soc. 129 (2007) 328–334.

[10] P. Ahuja, R. Sarkar, P.R. Vasos, G. Bodenhausen, Diffusion coefficients of biomolecules using long-lived spin states, J. Am. Chem. Soc. 131 (2009) 7498–7499.

[11] R. Sarkar, P. Ahuja, P.R. Vasos, G. Bodenhausen, Measurement of slow diffusion coefficients of molecules with arbitrary scalar couplings via long-lived spin states, ChemPhysChem 9 (2008) 2414–2419.

[12] J.-N. Dumez, J.T. Hill-Cousins, R.C.D. Brown, G. Pileio, Long-lived localization in magnetic resonance imaging, J. Magn. Reson. 246 (2014) 27–30.

[13] G. Pileio, J.-N. Dumez, I.-A. Pop, J.T. Hill-Cousins, R.C.D. Brown, Real-space imaging of macroscopic diffusion and slow flow by singlet tagging MRI, J. Magn. Reson. 252 (2015) 130–134.

[14] S. Cavaldini, P.R. Vasos, Singlet states open the way to longer time-scales in the measurement of diffusion by NMR spectroscopy, Concr. Magn. Reson. 32A (2008) 68–78.

[15] R. Buratto, D. Mammoli, E. Chiarparin, G. Williams, G. Bodenhausen, Exploring weak ligand-protein interactions by long-lived NMR states: improved contrast in fragment-based drug screening, Angew. Chem. Int. Ed. 53 (2014) 11376–11380.

[16] A. Bornet, S. Jannin, G. Bodenhausen, Three-field NMR to preserve hyperpolarized proton magnetization as long-lived states in moderate magnetic fields, Chem. Phys. Lett. 512 (2011) 151–154.

[17] P.R. Vasos, A. Comment, R. Sarkar, P. Ahuja, S. Jannin, J.-P. Ansermet, J.A. Konter, P. Hautle, B. van den Brandt, G. Bodenhausen, Long-lived states to sustain hyperpolarized magnetization, Proc. Natl. Acad. Sci. USA 106 (2009) 18469–18473.

[18] G. Pileio, S. Bowen, C. Laustsen, M.C.D. Tayler, J.T. Hill-Cousins, L.J. Brown, R.C.D. Brown, J.H. Ardenkjaer-Larsen, M.H. Levitt, Recycling and imaging of nuclear singlet hyperpolarization, J. Am. Chem. Soc. 135 (2013) 5084–5088.

[19] M.C.D. Tayler, I. Marco-Rius, M.I. Kettunen, K.M. Brindle, M.H. Levitt, G. Pileio, Direct enhancement of nuclear singlet order by dynamic nuclear polarization, J. Am. Chem. Soc. 134 (2012) 7668–7671.

[20] M.B. Franzoni, L. Buljubasich, H.W. Spiess, K. Münnemann, Long-lived ^{1}H singlet spin states originating from para-hydrogen in Cs-symmetric molecules stored for minutes in high magnetic fields, J. Am. Chem. Soc. 134 (2012) 10393–10396.

[21] M.B. Franzoni, D. Graafen, L. Buljubasich, L.M. Schreiber, H.W. Spiess, K. Münnemann, Hyperpolarized ^{1}H long lived states originating from parahydrogen accessed by RF irradiation, Phys. Chem. Chem. Phys. 15 (2013) 17233–17239.

[22] Y. Feng, T. Theis, X. Liang, Q. Wang, P. Zhou, W.S. Warren, Storage of hydrogen spin polarization in long-lived $^{13}C_2$ singlet order and implications for hyperpolarized magnetic resonance imaging, J. Am. Chem. Soc. 135 (2013) 9632–9635.

[23] W.S. Warren, E. Jenista, R.T. Branca, X. Chen, Increasing hyperpolarized spin lifetimes through true singlet eigenstates, Science 323 (2009) 1711–1714.

[24] A.S. Kiryutin, H. Zimmermann, A.V. Yurkovskaya, H.-M. Vieth, K.L. Ivanov, Long-lived spin states as a source of contrast in magnetic resonance spectroscopy and imaging, J. Magn. Reson. 261 (2015) 64–72.

[25] A.S. Kiryutin, K.L. Ivanov, A.V. Yurkovskaya, H.-M. Vieth, N.N. Lukzen, Manipulating spin hyper-polarization by means of adiabatic switching of RF-field, Phys. Chem. Chem. Phys. 15 (2013) 14248–14255.

[26] A.S. Kiryutin, A.V. Yurkovskaya, N.N. Lukzen, H.-M. Vieth, K.L. Ivanov, Exploiting adiabatically switched RF-field for manipulating spin hyperpolarization induced by parahydrogen, J. Chem. Phys. 143 (2015) 234203.

[27] M.H. Levitt, Symmetry constraints on spin dynamics: application to hyperpolarized NMR, J. Magn. Reson. 262 (2015) 91–99.

[28] B. Meier, J.-N. Dumez, G. Stevanato, J.T. Hill-Cousins, S.S. Roy, P. Håkansson, S. Mamone, R.C.D. Brown, G. Pileio, M.H. Levitt, Long-lived nuclear spin states in methyl groups and quantum-rotor-induced polarization, J. Am. Chem. Soc. 135 (2013) 18746–18749.

[29] Software for Optimizing Parameters for APSOC and SOS-filter. <http://www.tomo.nsc.ru/en/nmr/sos-filter/>.

[30] S.J. DeVience, R.L. Walsworth, M.S. Rosen, Preparation of nuclear spin singlet states using spin-lock induced crossing, Phys. Rev. Lett. 111 (2013) 173002.

[31] T. Theis, Y. Feng, T. Wu, W.S. Warren, Composite and shaped pulses for efficient and robust pumping of disconnected eigenstates in magnetic resonance, J. Chem. Phys. 140 (2014) 014201.

[32] S.J. DeVience, R.L. Walsworth, M.S. Rosen, Dependence of nuclear spin singlet lifetimes on RF spin-locking power, J. Magn. Reson. 218 (2012) 5–10.

[33] G. Pileio, M. Carravetta, M.H. Levitt, Storage of nuclear magnetization as long-lived singlet order in low magnetic field, Proc. Natl. Acad. Sci. USA 107 (2010) 17135–17139.

[34] A.N. Pravdivtsev, A.V. Yurkovskaya, N.N. Lukzen, H.-M. Vieth, K.L. Ivanov, Exploiting Level Anti-Crossings (LACs) in the rotating frame for transferring spin hyperpolarization, Phys. Chem. Chem. Phys. 16 (2014).

[35] Y. Feng, R.M. Davis, W.S. Warren, Accessing long-lived nuclear singlet states between chemically equivalent spins without breaking symmetry, Nat. Phys. 8 (2012) 831–837.

[36] J. Natterer, J. Bargon, Parahydrogen induced polarization, Prog. Nucl. Mag. Res. Sp. 31 (1997) 293–315.

[37] R.A. Green, R.W. Adams, S.B. Duckett, R.E. Mewis, D.C. Williamson, G.G.R. Green, The theory and practice of hyperpolarization in magnetic resonance using parahydrogen, Prog. Nucl. Magn. Reson. Spectrosc. 67 (2012) 1–48.

[38] N.A. Gershenfeld, I.L. Chuang, Bulk spin-resonance quantum computation, Science 275 (1997) 350–356.

[39] M.A. Nielsen, I.L. Chuang, Quantum Computation and Quantum Information, Cambridge University Press, Cambridge, UK, 2002.